Tree lifespans in a warming world: unveiling the universal trade-off between growth and lifespan in temperate forests

SUPPORTING INFORMATION

Table S1. The results of principal component analysis of nine climate variables. The first component (PC1) explained more than 60% of the variance. PC1 was multiplied by −1 in subsequent multiple linear regression analysis.

	PC1(66.2%)
Mean annual temperature (MAT)	-0.39
Mean diurnal range (MDR)	0.32
Temperature seasonality (TS)	0.35
Temperature of the warmest quarter (MTWQ)	-0.32
Temperature of the coldest quarter (MTCQ)	-0.39
Annual precipitation (AP)	-0.36
Precipitation seasonality (PS)	0.16
Precipitation of the wettest quarter (PWQ)	-0.33
Precipitation of the driest quarter (PDQ)	-0.32

Table S2. Three models were devised for forecasting future growth and lifespan. Model1 predicts future growth under future environments, model2 predicts future lifespan under future environments, and model3 predicts future lifespan considering both future environments and growth-lifespan trade-off.

Model1	**Early growth rate** ~ MAT + MDR + TS + MTWQ + MTCQ + AP + PS + PWQ + PDQ + HM + Altitude
Model2	**Lifespan** ~ MAT + MDR + TS + MTWQ + MTCQ + AP + PS + PWQ + PDQ + HM + Altitude
Model3	**Lifespan** ~ MAT + MDR + TS + MTWQ + MTCQ + AP + PS + PWQ + PDQ + HM + Altitude **+** Early growth rate

Table S3. The coefficient of determination (R^2) from three random forest regression models that iterated 20 times. Details of the three models can be found in supplementary Table S2.

	Model1	**Model2**	**Model3**
Iteration1	0.47	0.43	0.51
Iteration2	0.23	0.45	0.58
Iteration3	0.38	0.29	0.29
Iteration4	0.36	0.18	0.30
Iteration5	0.20	0.13	0.30
Iteration6	0.23	0.46	0.51
Iteration7	0.49	0.59	0.69
Iteration8	0.43	0.45	0.49
Iteration9	0.39	0.20	0.44
Iteration10	0.20	0.08	0.15
Iteration11	0.37	0.24	0.49
Iteration12	0.28	0.25	0.19
Iteration13	0.39	0.51	0.62
Iteration14	0.26	0.21	0.32
Iteration15	0.22	0.20	0.39
Iteration16	0.08	0.21	0.32
Iteration17	0.34	0.36	0.45
Iteration18	0.53	0.36	0.39
Iteration19	0.30	0.41	0.51

Iteration20	0.50	0.41	0.50
Mean	**0.33**	**0.32**	**0.42**

Table S4. Effect of mean environmental conditions, and their spatial variation on trade-off strength. Environmental variation was calculated as the range of environmental variables for each species and metacommunity. Values are Pearson correlation coefficients between each variable and trade-off strength, and bold values represent significant correlations ($p < 0.05$).

	Within species' trade-off strength		Within communities' trade-off strength	
	Environment condition	Environment heterogeneity	Environment condition	Environment heterogeneity
Altitude	0.37	**0.47**	0.25	0.10
Human pressure	**-0.45**	0.33	**-0.35**	-0.23
Mean annual temperature	**-0.66**	**0.55**	**-0.38**	0.19
Mean diurnal range	**0.60**	**0.60**	**0.46**	0.29
Temperature seasonality	**0.63**	**0.54**	0.27	-0.11
Temperature of the warmest quarter	**-0.59**	**0.54**	**-0.40**	**0.32**
Temperature of the coldest quarter	**-0.62**	**0.56**	**-0.33**	0.15
Annual precipitation	**-0.60**	**0.48**	**-0.37**	-0.08
Precipitation seasonality	0.13	**0.54**	**0.39**	**0.42**

Precipitation of the wettest quarter	**-0.58**	0.35	-0.25	-0.14
Precipitation of the driest quarter	**-0.55**	0.34	**-0.34**	-0.10

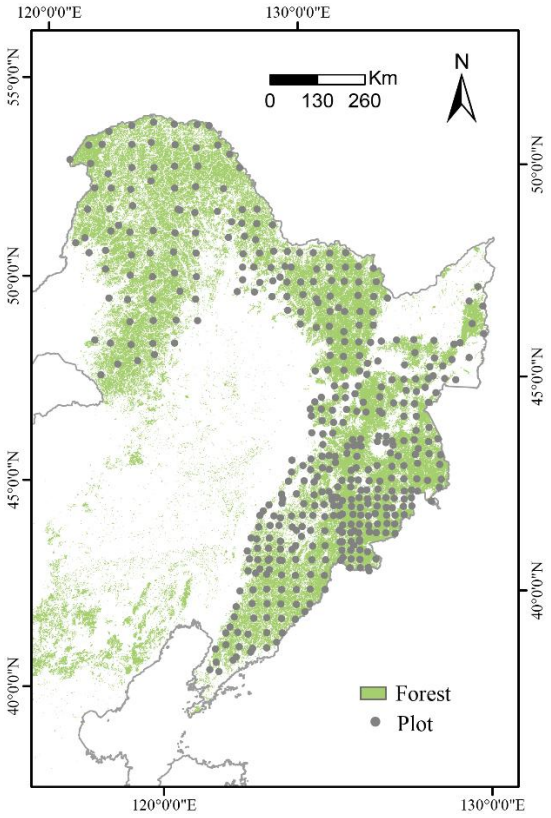

Figure S1. Geographical distributions of the 445 sampled plots utilized in this study.

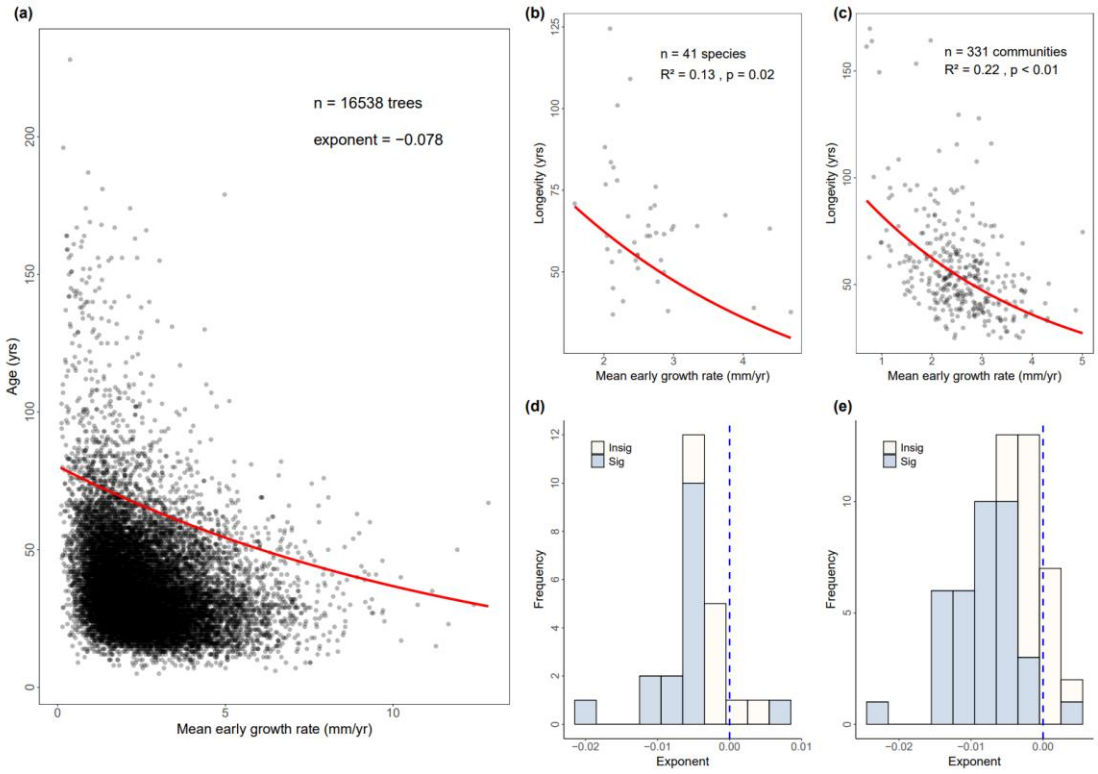

Figure S2. Trade-offs between early growth rate and lifespan at multiple levels, excluding plots with a human pressure index ≥ 0.5. Panels (a), (b), and (c) show the relationship between tree early growth rate and lifespan across (a) 16538 trees, (b) 41 species, and (c) 331 plots, with red lines indicating nonlinear regression trends. Panels (d) and (e) show the distribution of exponents from the relationship between early growth rate and lifespan (d) within each species and (e) within each metacommunity, with the blue dashed line representing the exponent value of 0, and Sig and Insig indicate significant relationships ($p < 0.05$) and insignificant relationships ($p > 0.05$), respectively.

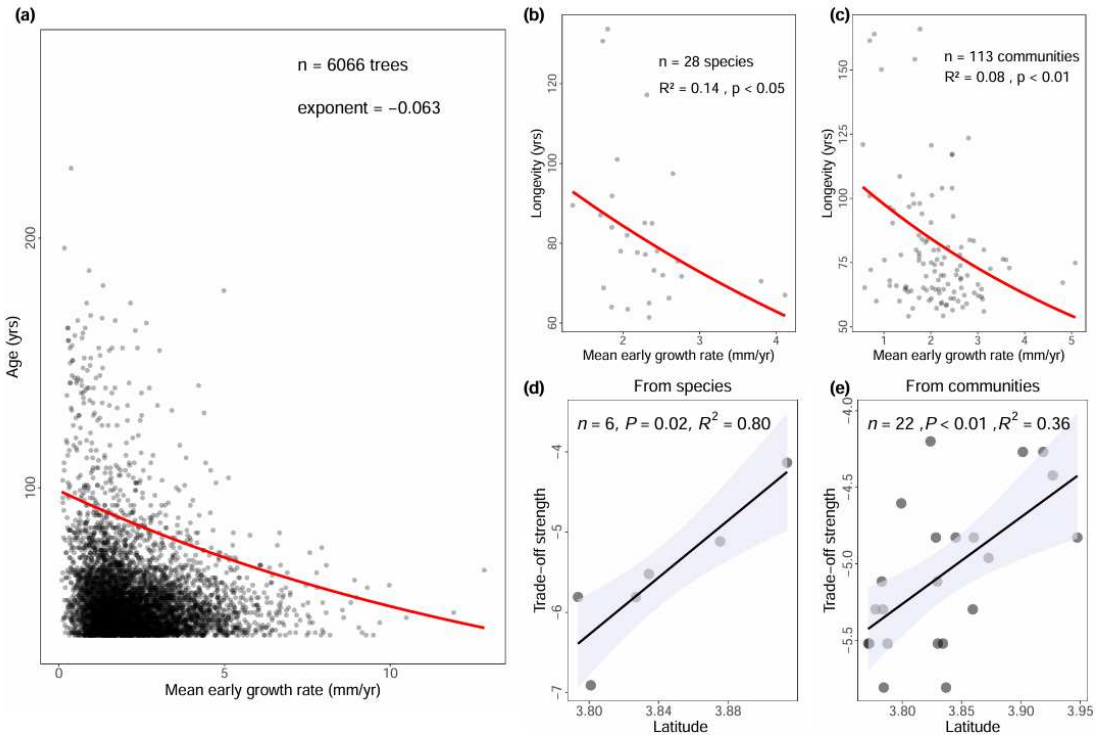

Figure S3. Trade-offs between early growth rate and lifespan at multiple levels, excluding trees younger than 40 years. Panels (a), (b), and (c) show the relationship between tree early growth rate and lifespan across (a) 6066 trees, (b) 28 species, and (c) 113 plots, with red lines indicating nonlinear regression trends. Panels (d) and (e) show the latitudinal patterns of trade-off strength from (d) species and (e) communities, with trade-off strength from species and latitude transformed to meet the normality.

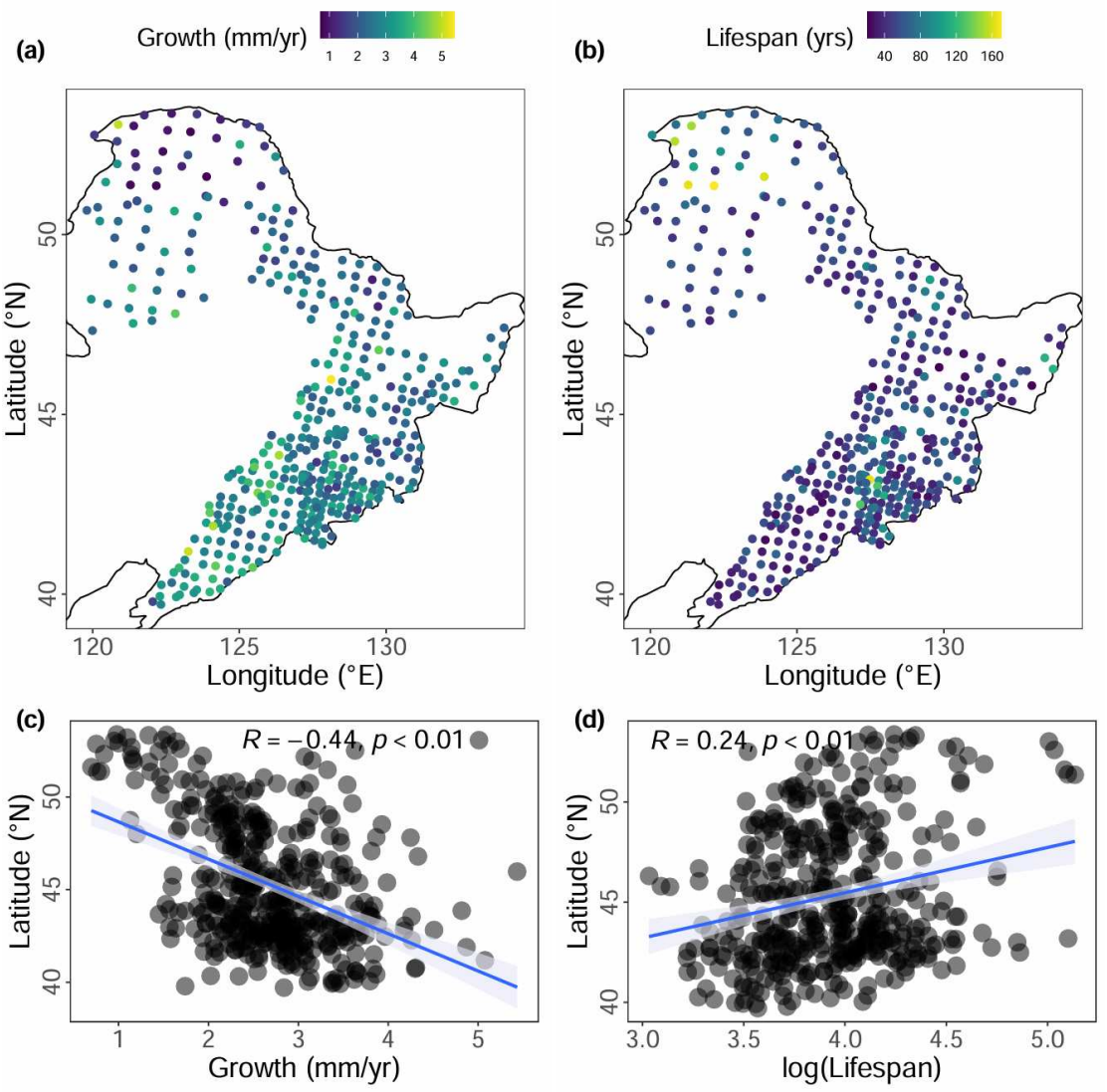

Figure S4. Latitudinal patterns of tree early growth rate and lifespan across 417 communities. The upper panel shows the geographical distributions of (a) tree early growth rate and (b) lifespan. The lower panel shows the correlation relationships between latitude and (c) tree early growth rate and (d) lifespan.

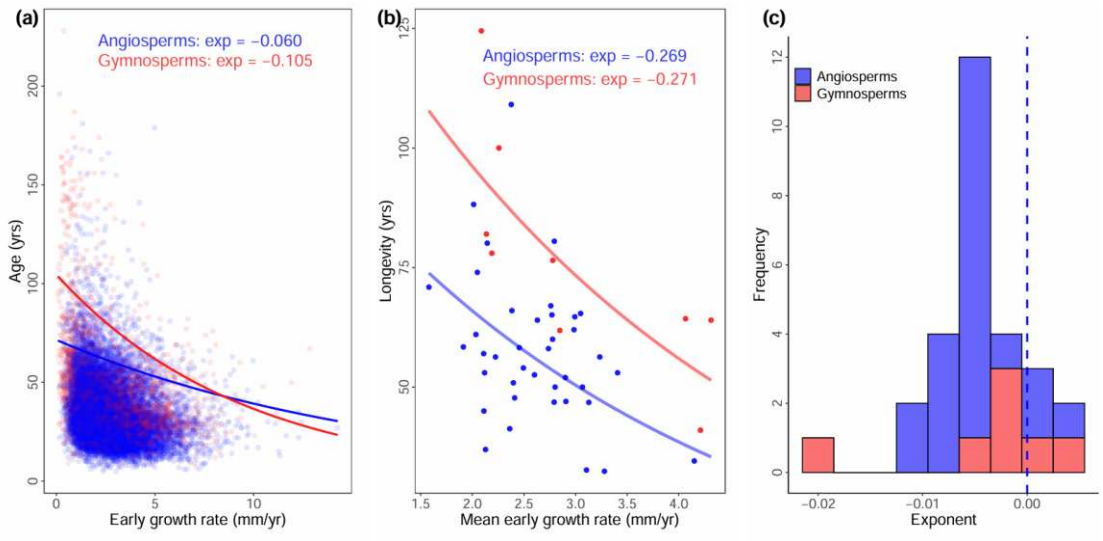

Figure S5. Trade-offs between early growth rate and lifespan in angiosperms and gymnosperms at multiple levels. Panel (a) shows the relationship between tree early growth rate and lifespan across all trees. Panel (b) shows the relationship between tree early growth rate and lifespan across all species. Panel (c) shows the distribution of exponent from the relationship between early growth rate and lifespan within each species, with the blue dashed line showing the exponent value of 0, and each exponent value extracted from significant relationships between early growth rate and lifespan.

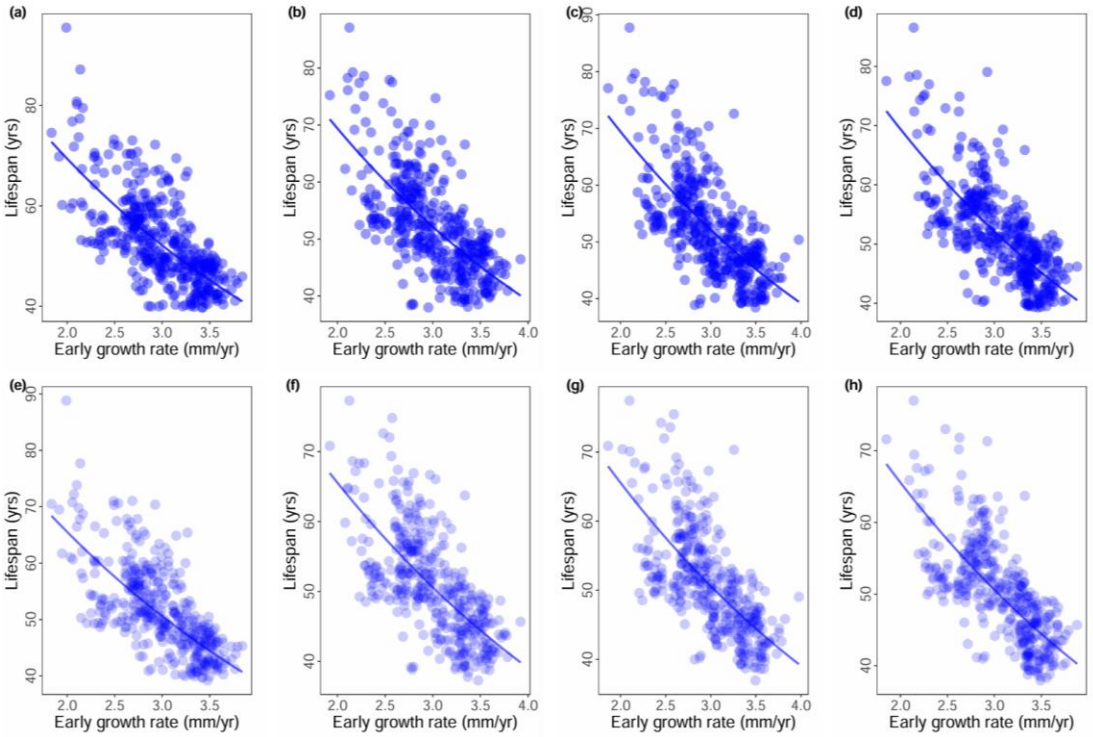

Figure S6. Early growth rate, lifespan, and their trade-off at the community level under the future climate scenarios, from Shared Socio-economic Pathways (SSP) 1-2.6 (a, e), SSP 2-4.5 (b, f), SSP 3-7.0 (c, g) and SSP 5-8.5 (d, h), using the model MRI-ESM2-0 in the 2050s. Lifespans in panels (a, b, c, d) are environmental-driven, and lifespans in panels (e, f, g, h) are affected by both environments and the growth-lifespan trade-off.

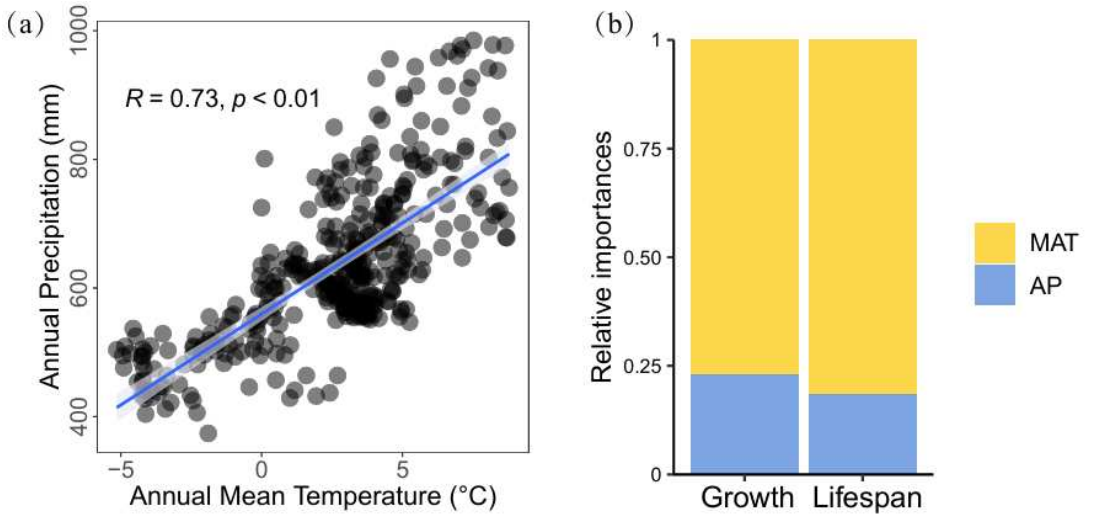

Figure S7. The covariation between temperature and precipitation within our study area (a), and the relative importance of temperature and precipitation on growth and lifespan (b). We assessed the relative importance of temperature and precipitation by decomposing R^2 to ascertain the proportion contributed by each variable in the multiple linear model. MAT: annual mean temperature; AP: annual precipitation.

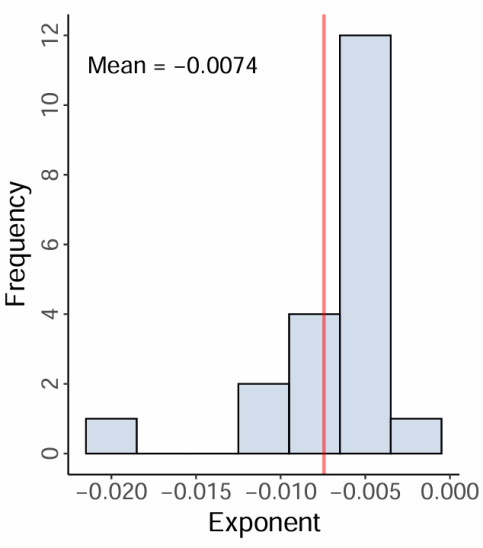

Figure S8. The distribution of exponents from the significant trade-off between relative early growth rate and relative lifespan within each of the 20 species. The mean exponent value was calculated by weighting the cube root of each species' abundance, and the red line in the plot represents this mean exponent value. This mean exponent value is similar to the mean exponent value from global temperate forests (Brienen et al., 2020).

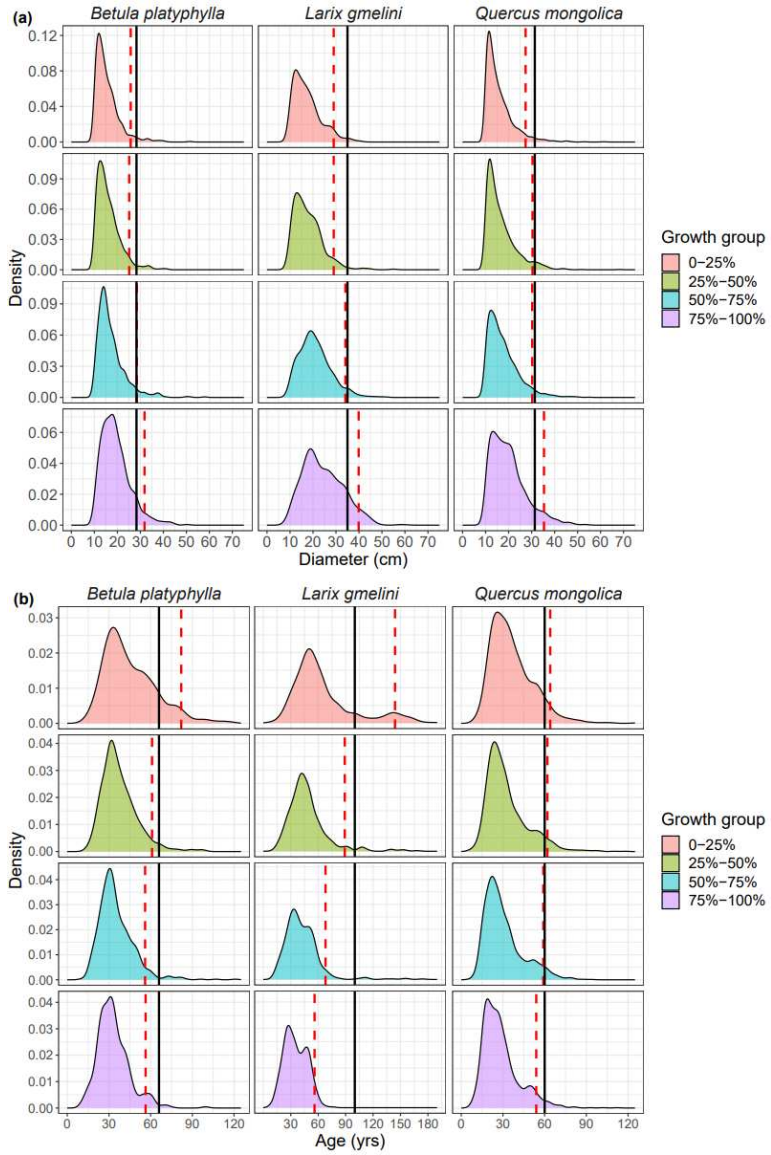

Figure S9. Distributions of (a) tree size and (b) tree age for four early growth rate groups for three species, *Betula platyphylla*, *Larix gmelini* and *Quercus mongolica*, chosen for their large sample sizes. Each growth rate group represents a specific percentile range of early growth rates, with higher percentiles indicating faster early growth rates. The black line represents the 95th percentile of tree size and age across all individuals for each species, and the red line shows the 95th percentile of tree size and age for each growth group within the species.

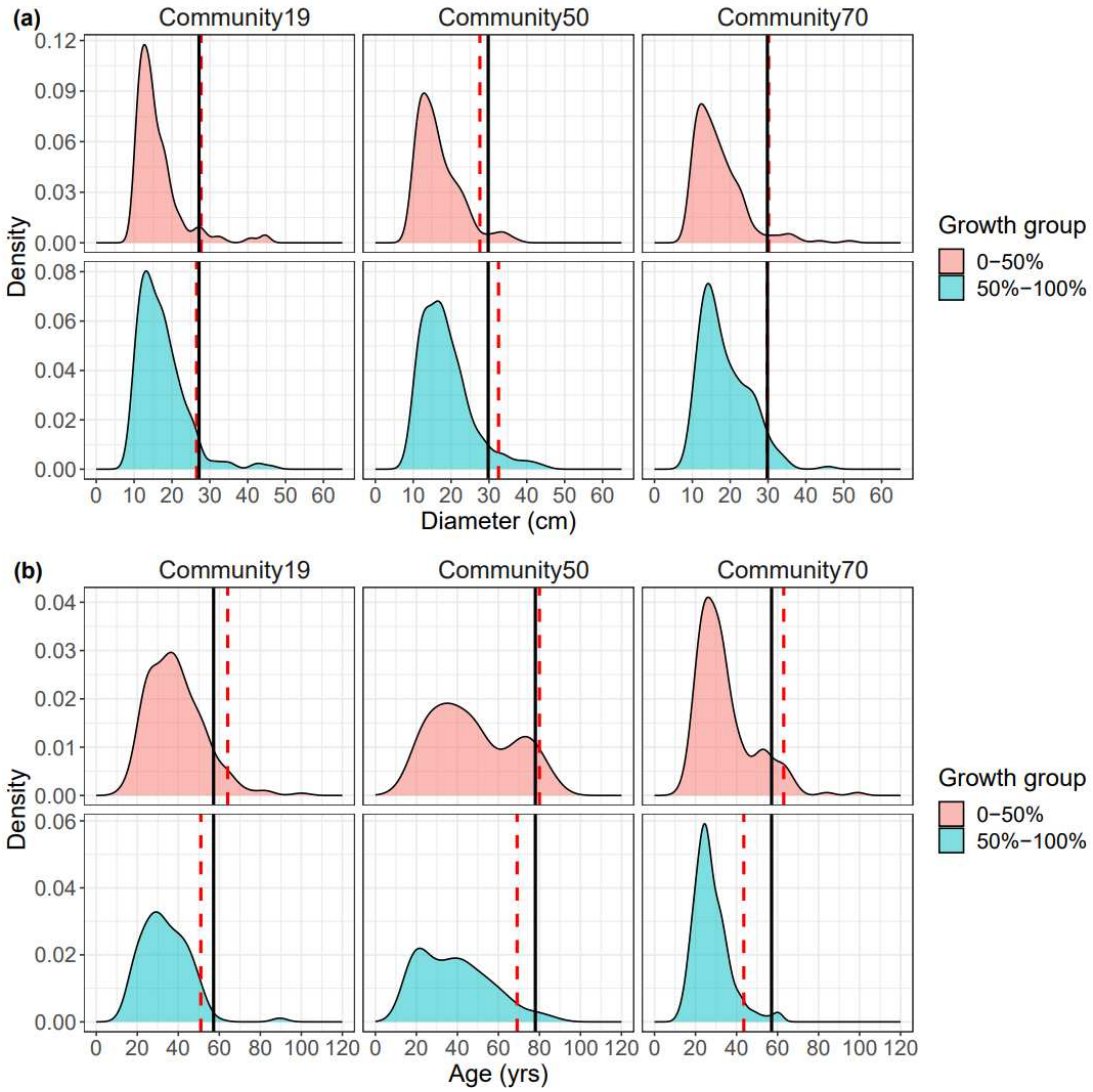

Figure S10. Distributions of (a) tree size and (b) tree age for two early growth rate groups for three metacommunities, selected based on their large sample sizes for analysis. Each growth rate group represents a specific percentile range of early growth rates, with higher percentiles indicating faster early growth rates. The black line represents the 95th percentile of tree size and age across all individuals for each metacommunity, and the red line shows the 95th percentile of tree size and age for each growth group within the metacommunity.

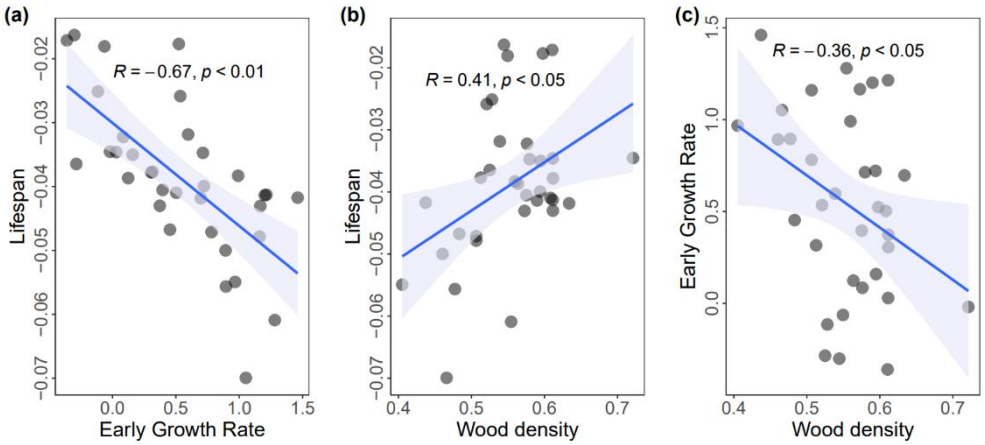

Figure S11. Relationships between early growth rate, lifespan, and wood density for *Larix gmelini*. Early growth rate and lifespan were derived for each site, based on data from more than 20 individuals per plot. Wood density was measured from a single randomly selected individual in each plot. Lifespan and early growth rate were transformed to meet the normality requirements of data analysis.

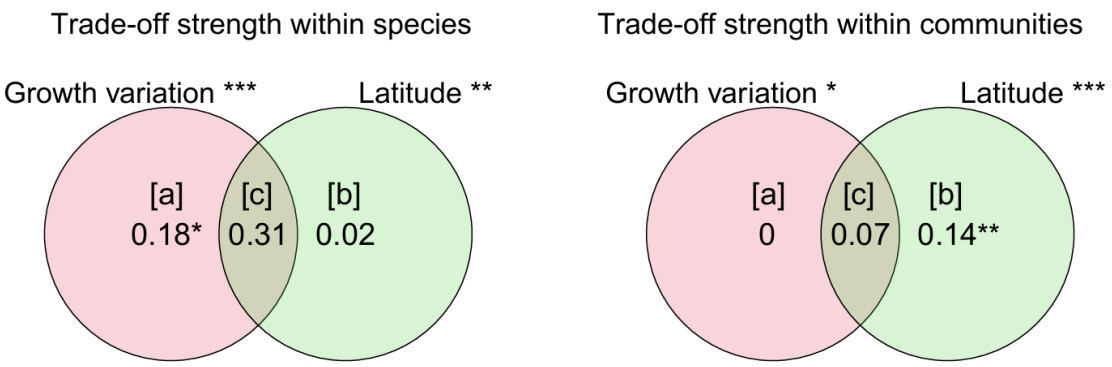

Figure S12. The Venn diagrams represent the partitioning of the variance in the trade-off strength. The fraction [a] signifies the variance in trade-off strength explained by growth variation independently, fraction [b] represents the variance explained by latitude independently, and fraction [c] is the variance explained jointly by growth variation and latitude. The left panel indicates that the trade-off strength within species is not significantly explained by latitude independently but rather by growth variation alone and by the shared effect of growth variation and latitude. The right panel shows that the trade-off strength within communities is not explained by growth variation independently, but by latitude independently and the shared effect of growth variation and latitude.

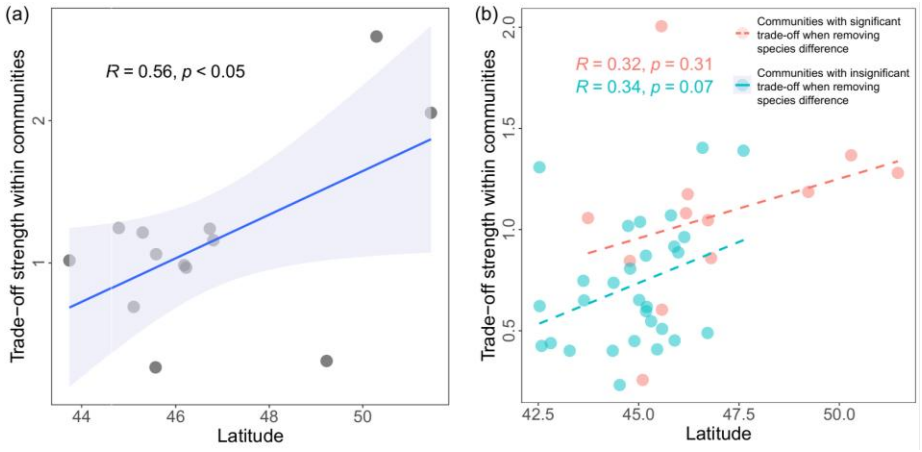

Figure S13. Latitudinal patterns of within-community trade-off strength with (a) and without (b) controlling for species variation. In (a), trade-off strength is recalculated by standardizing age and growth values as relative values within species to remove interspecific variation. Specifically, age is expressed as age divided by the maximum age within each species, and growth as growth divided by the maximum growth within each species. In (b), latitudinal trends of within-community trade-offs are shown without controlling for species variation. Red points represent communities that exhibited significant trade-offs after controlling for species variation, while blue points represent communities with nonsignificant trade-offs after controlling for species variation.

Reference

Brienen, R. J. W., Caldwell, L., Duchesne, L., Voelker, S., Barichivich, J., Baliva, M., Ceccantini, G., Di Filippo, A., Helama, S., Locosselli, G. M., Lopez, L., Piovesan, G., Schöngart, J., Villalba, R., & Gloor, E. (2020). Forest carbon sink neutralized by pervasive growth-lifespan trade-offs. *Nature Communications*, *11*(1), 4241. https://doi.org/10.1038/s41467-020-17966-z